

## **Authors' Replies to Review**

Dear editor,

We have very much appreciated the review by Kevin Lepot and we have revised the text as suggested. Below, we are responding stepwise to the comments made the reviewer (our answers are given in italics). We send you a new version of the manuscript, where we again highlighted (by tracking changes in the reviewing mode) all the changes.

On behalf of the authors

Josef Elster

### **Reviewer #1:**

L271 – particles incorporated within filaments – this is not shown in the data. The particles are incorporated in the biofilm, not the filaments.

*Corrected.*

L428 – add “nanostructured” carbonates

*Corrected.*

L390-395 “elevated mount of mineral grains” = elevated is exaggerated, the mineral grains are only sparse, they do not bury the mats under clastic layers!

“soft mineral matter” has no meaning unless you compare mineral hardness, which is not the case as you include soft minerals and hard quartz. Please change to “mixture of organic matter and mineral clasts”

*Corrected.*

Lines 289+743 = with a cyanobacterial filament = add “possible cyanobacterial filament”, as you did not observe the cyanobacteria, only a tube that suggests its possible presence

*Corrected.*

L280-284 + caption Fig. 9 = remove reference to corrosion and recrystallization here only to describe textures morphologically; then please discuss recrystallization versus primary mesostructured carbonate structure in discussion, leaving open both possibilities in caption & result section.

*References to corrosion and recrystallization were removed from Results and Figure captions, the discussion leaves open (L 422-429) the two possibilities of origin of the observed structures.*

# Unusual biogenic calcite structures in two shallow lakes, James Ross Island, Antarctica

J. Elster<sup>1,2\*</sup>, L. Nedbalová<sup>2,3</sup>, R. Vodrážka<sup>4</sup>, K. Láska<sup>5</sup>, J. Haloda<sup>4</sup>, J. Komárek<sup>1,2</sup>

[1] {Centre for Polar Ecology, Faculty of Science, University of South Bohemia, Na Zlaté Stoce 3, 37005 České Budějovice, Czech Republic}

[2] {Institute of Botany, Academy of Sciences of the Czech Republic, Dukelská 135, 37982 Třeboň, Czech Republic}

[3] {[Department of Ecology](#), Faculty of Science, Charles University in Prague, Albertov 6, 12843 Prague, Czech Republic}

[4] {Czech Geological Survey, Klárov 3, 11821 Prague, Czech Republic}

[5] {[Department of Geography](#), Faculty of Science, Masaryk University ~~in Brno~~, Kotlářská 2, 61137 Brno, Czech Republic}

Correspondence to: J. Elster (jelster@prf.jcu.cz)

## Abstract

The floors of two shallow endorheic lakes, located on volcanic surfaces on James Ross Island, are covered with calcareous organosedimentary structures. Their biological and chemical composition, lake water characteristics, and seasonal variability of the thermal regime are introduced. The lakes are frozen down to the bottom eight-nine months per year and their water chemistry is characterized by low conductivity and neutral to slightly alkaline pH. The photosynthetic microbial mat is composed of filamentous cyanobacteria and microalgae that are considered to be Antarctic endemic species. The mucilaginous black biofilm is covered by green spots formed by a green microalga and the macroscopic structures are packed together with fine material. Thin sections consist of rock substrate, soft biofilm, calcite spicules and mineral grains originating from different sources. The morphology of the spicules is typical of calcium carbonate monocrystals having a layered structure and specific surface texture, which

30 reflect growth and degradation processes. The spicules chemical composition and structure  
31 correspond to pure calcite. Lakes age, altitude, morphometry, geomorphological and  
32 hydrological stability, including low sedimentation rates, together with thermal regime  
33 predispose the existence of this community. We hypothesize that the precipitation of calcite is  
34 connected with the photosynthetic activity of the green microalgae that were not recorded in  
35 any other lake in the region. This study has shown that the unique community producing  
36 biogenic calcite spicules is quite different to any yet described.

37

## 38 **1 Introduction**

39 The floors of most Antarctic lakes are covered with photosynthetic microbial mats (Vincent  
40 and Laybourn-Parry, 2008). However, the degree of disturbance plays a key role in the  
41 development of microbial mats. When growing in low-disturbance habitats, interactions  
42 between benthic microbial communities and their environments can produce complex  
43 emergent structures. Such structures are best developed in extreme environments, including  
44 benthic communities of deep, perennially ice-covered Antarctic lakes, where physical and  
45 chemical conditions, and/or geographical isolation preclude the development of larger  
46 organisms that could otherwise disrupt organised microbial structures (Wharton, 1994;  
47 Andersen et al., 2011). Many organosedimentary structures that emerge in these conditions  
48 are laminated and accrete through episodic trapping of sediments or grains and precipitation  
49 of minerals within a growing biogenic matrix (e.g. Arp et al., 2001; Reid et al., 2003). In  
50 perennially ice-covered lakes, the seasonality of growth imposed by the summer-winter light-  
51 dark conditions can induce annual growth laminations (Hawes et al., 2001), reinforced by  
52 calcite precipitation during growth and sediment diagenesis (Wharton et al., 1982; Wharton,  
53 1994; Sutherland and Hawes, 2009). Calcite precipitation is not, however, a prerequisite for  
54 laminated, stromatolite-like communities (Walter, 1976; Schieber, 1999; Yamamoto et al.,  
55 2009). A diversity of micro- to nanostructured  $\text{CaCO}_3$  associated with extracellular polymeric  
56 substances and prokaryotes was described from the sediments of an East Antarctic lake (Lepot  
57 et al, 2014). There is also a growing experimental evidence that some carbonate precipitates  
58 are only produced in the presence of organic matter (Cölfen and Antonietti, 1998; Pedley et  
59 al., 2000).

60 Precipitation of calcite by expulsion (segregation) is also a common process in the nature  
61 related to the freezing of common low ionic strength  $\text{Ca}^{2+}$  -  $\text{HCO}_3^-$  waters. Calcite  
62 precipitation related to water freezing was observed and described also from various polar-

63 alpine settings, e.g. from lake bottoms of Dry Valleys in Antarctica (Nakai et al., 1975) or as a  
64 results of aufeis (icing, naled) formation in Northern Canada (Clark and Lauriol, 1997).  
65 Crystalline precipitates that form subglacially on bedrock were reported from numerous  
66 locations (Ng and Hallet, 2002), for example fine-grained calcite powders were observed in  
67 subglacial deposits and in aufeis formations, Svalbard (Wadham et al., 2000) or in basal ice  
68 and subglacial clastic deposits of continental glaciers of Switzerland (Fairchild et al., 1993).  
69 Calcite pendants occurred beneath coarse clasts in well-drained sediments on Svalbard  
70 (Courty et al., 1994) and calcite coatings were found in cavities in cold-climate Pleistocene  
71 deposits of Western Transbaikalia, Russia, and in modern surface deposits at Seymour Island,  
72 Antarctica (Vogt and Corte, 1996).

73 James Ross Island belongs to a transitory zone between the maritime and continental  
74 Antarctic regions (Øvstedal and Lewis Smith, 2001). Air temperature records indicate  
75 progressive warming trends from 1.5 °C to 3.0 °C over the Antarctic Peninsula during the past  
76 50 years (Turner et al., 2014). More than 80% of the island surface is covered with ice  
77 (Rabassa et al., 1982). Only the northernmost part of the island, the Ulu Peninsula, is  
78 significantly deglaciated and represents one of the largest ice-free areas in the northern part of  
79 the Antarctic Peninsula. The origin of the lakes on James Ross Island is related to the last  
80 glaciations of the Antarctic Peninsula ice sheet and retreat of the James Ross Island ice cap  
81 during the late Pleistocene and Holocene (Nývlt et al., 2011; Nedbalová et al., 2013).  
82 Interactions between volcanic landforms and glacial geomorphology during previous glacial-  
83 interglacial cycles, the Holocene paraglacial and periglacial processes and relative sea level  
84 change have resulted in the complex present-day landscape of James Ross Island (Davies et  
85 al., 2013). All of these processes have influenced the development of the lakes which are  
86 found on the Ulu Peninsula at altitudes from <20 m above sea level (a.s.l.) near the coast to  
87 400 m a.s.l. in the mountain areas (Nedbalová et al., 2013).

88 During two Czech research expeditions (2008 and 2009) to James Ross Island, lake  
89 ecosystems of the Ulu Peninsula were studied in respect to their origin, morphometry,  
90 physical, chemical and biological characteristics (Nedbalová et al., 2013), together with  
91 detailed cyanobacterial and microalgal diversity descriptions (Komárek and Elster, 2008;  
92 Komárek et al., 2011; Kopalová et al., 2013; Škaloud et al., 2013; Komárek et al., 2015). As  
93 part of this study, we encountered 1 to 5 millimetres scale calcareous organosedimentary  
94 structures on the floor of two endorheic lakes, 1 and 2, which are quite different to any  
95 microbially mediated structures yet described from modern environments. These shallow

96 lakes on higher-lying levelled surfaces originated after the deglaciation of volcanic mesas  
97 which became ice-free some 6.5–8 ka ago (Johnson et al., 2011) and are considered among  
98 one of the oldest in the region. However, a later appearance of these lakes is also possible, as  
99 we have no exact dates from their sediments (Nedbalová et al., 2013).

100 The aim of this paper is to describe in detail the chemical and biological composition of the  
101 organosedimentary structures together with the limnological characteristics of the two lakes.  
102 A hypothesis concerning the formation of calcite spicules is also presented. The results of this  
103 study can serve as a baseline for understanding microbial behaviors in forming these  
104 organosedimentary structures, which will provide insight into the interpretation of fossil  
105 forms from early Earth.

106

## 107 **2 Materials and methods**

### 108 **2.1 Study site**

109 Endorheic lake 1 (63°54'11.7" S, 57°46'49.9" W, altitude 65 m a.s.l.) and endorheic lake 2  
110 (63°53'54.6" S, 57°46'33.8" W, altitude 40 m a.s.l.) are shallow lakes located near Andreassen  
111 Point on the E coast of the deglaciated Ulu Peninsula, in the northern part of James Ross  
112 Island, NE Antarctic Peninsula (Figure 1). They are shallow with maximum depth of 1.1 and  
113 0.9 m, and mean depth of 0.5 and 0.3 m. Their catchment areas are 0,340 and 0,369 km<sup>2</sup>, lake  
114 area 4220 and 2970 m<sup>2</sup> and water volume 2183 and 1037 m<sup>3</sup>, respectively (Nedbalová et al.,  
115 2013). Melt water from the surrounding snowfields feed the lakes for a few weeks during the  
116 austral summer. The water level in both lakes fluctuated dramatically. Water is mainly lost  
117 through evaporation from the ice free water surface. During this period, intense evaporation in  
118 both lakes is coupled with macroscopic changes in the littoral belt. The extent of water level  
119 fluctuation was documented for lake 1 (Figure 2).

120 Climate conditions of the Ulu Peninsula are characterized by mean annual air temperatures  
121 around –7 °C and mean summer temperatures above 0 °C for up to four months (Láska et al.,  
122 2011a). The mean global solar radiation is around 250 W m<sup>-2</sup> in summer (December-  
123 February), with large day-to-day variation affected by extended cyclonic activity in the  
124 circumpolar trough and orographic effects over the Antarctic Peninsula (Láska et al., 2011b).  
125 The bedrock is composed of two main geological units, namely Cretaceous back-arc basin  
126 sediments and mostly subglacial Neogene to Quaternary volcanic rocks (Olivero et al., 1986).

127 The terrestrial vegetation is limited to non-vascular plants and composed predominantly of  
128 lichen and bryophyte tundra. A large number of lakes can be found in this area, formed by  
129 glacial erosion and deposition, followed by glacier retreat during the Holocene (Nedbalová et  
130 al., 2013).

## 131 **2.2 Sampling procedures**

132 Lake 1 was sampled on 22 February 2008. In 2009, lake 1 was sampled on 5 January, lake 2  
133 on 12 January. Air temperature at 2 m above ground was measured by an automatic weather  
134 station (AWS) located nearby (Figure 1). Incident global solar radiation was monitored with a  
135 LI-200 pyranometer (LI-COR, USA) at Mendel Station, located 11 km northwest of the study  
136 site (Figure 1). The LI-200 spectral response curve covers wavelengths from 400 to 1100 nm  
137 with absolute error typically of  $\pm 3\%$  under natural daylight conditions. Global radiation was  
138 measured at 10s time interval and stored as 30-min average values, while air temperature was  
139 recorded at 1 hour intervals from 1 February 2009 to 30 November 2010. In lake 1, water  
140 temperature was monitored from 10 February 2009 to 30 November 2010 at 1 hour intervals  
141 using a platinum resistance thermometer with Minikin T data logger (EMS Brno, Czech  
142 Republic) installed on the lake bottom.

143 Conductivity, pH, temperature and dissolved oxygen were measured in situ with a portable  
144 meter (YSI 600) at the time the lakes were ice free. Water samples were collected from the  
145 surface layer, immediately filtered through a 200- $\mu\text{m}$  polyamide sieve to remove zooplankton  
146 and coarse particles. Chlorophyll-a was extracted from particles retained on Whatman GF/F  
147 glass microfiber filters according to Pechar (1987). After centrifugation, chlorophyll-a was  
148 measured by a Turner TD-700 fluorometer equipped with a non-acidification optical kit. The  
149 remaining water was kept frozen until analyzed at the Institute of Hydrobiology (Czech  
150 Republic). The chemical analytical methods are given in Nedbalová et al. (2013). The stones  
151 covered by photoautotrophic mats – biofilm collected in the field were transported to the  
152 Czech Republic in a frozen and/or dry state, documented with stereomicroscope (Bresser, HG  
153 424018) and imaging fluorometer (FluorCam, PSI) and used for a) phytobenthos community  
154 description and isolation of dominant species, b) fix for thin section analyses, c) scanning  
155 electron and optical microscopy, and d) determination of the structure and chemical  
156 composition of calcium carbonate spicules.

### 157 **2.3 Thin section analyses**

158 Thin section analyses were made to observe both rock substrate and inorganic particles within  
159 biofilms. Dry microbial mat were saturated with epoxy resins in vacuum, subsequently cut  
160 perpendicularly and saturated again with epoxy resin. The sample was cemented to a glass  
161 slide after grinding and polishing, and a thin section was prepared by final sectioning,  
162 grinding and polishing to a desired thickness of 50–55  $\mu\text{m}$ . Thin sections of rocks were  
163 studied in transmitted (PPL) and polarized (XPL) light (Olympus BX-51M) and documented  
164 in transmitted light of a Nikon SMZ-645 optical microscope using NIS-Elements software.

### 165 **2.4 Biofilm scanning electron and optical microscopy**

166 The morphology of photoautotrophic mats and calcareous spicules was studied using standard  
167 methods of scanning electron microscopy (SEM) using back-scattered electrons (BSE) (Jeol  
168 JSM-6380, Faculty of Science, Charles University) and optical microscopy (Nikon SMZ-645  
169 using NIS-Elements software). Calcareous spicules were collected directly from the surface of  
170 biofilms. Samples studied in SEM were completely dried for 5 months at room temperature,  
171 then mounted on stubs with carbon paste and coated with gold prior to photomicrographing.

### 172 **2.5 Structure and chemical composition of calcium carbonate spicules – EDS** 173 **and EBSD analyses**

174 The chemical composition of the analyzed spicules was measured by using the Link ISIS 300  
175 system with 10  $\text{mm}^2$  Si-Li EDS detector on a CamScan 3200 scanning electron microscope  
176 (Czech Geological Survey, Prague). Analyses were performed using an accelerating voltage  
177 of 15 kV, 2 nA beam current, 1  $\mu\text{m}$  beam size and ZAF correction procedures. Natural  
178 carbonate standards (calcite, magnesite, rhodochrosite, siderite and smithsonite) were used for  
179 standardization. Subsequent structural identification was confirmed by electron backscattered  
180 diffraction (EBSD). Identification data and crystallographic orientation measurements were  
181 performed on the same scanning electron microscope using an Oxford Instruments Nordlys S  
182 EBSD detector. The thick sections used for EBSD applications were prepared by the process  
183 of chemo-mechanical polishing using colloidal silica suspension. The acquired EBSD patterns  
184 were indexed within Channe 15 EBSD software (Schmidt and Olensen, 1989) applying calcite  
185 and aragonite crystallographic models (Effenberger et al., 1981; Caspi et al., 2005).  
186 Orientation contrast images were collected from a 4-diodes forescatter electron detector

187 (FSD) integrated into the Nordlys S camera. EBSD pattern acquisition was carried out at 20  
188 kV acceleration voltage, 3 nA beam current, 33 mm working distance and 70° sample tilt.

189

## 190 **3 Results**

### 191 **3.1 General description of the lakes and water chemistry**

192 Pictures and detailed bathymetric parameters of both lakes together with marked lines of  
193 water level and the maximum extent of the photosynthetic microbial mat littoral belt in lake 1  
194 are presented in Figure 2.

195 The physico-chemical characteristics of the lake water for both lakes are given in Table 1.  
196 The sampling of lake 1 (pH 7.4–7.9, saturation of oxygen 98.9 %) was performed during  
197 cloudy days. Oxygen supersaturation (128%) together with a relatively high pH (8.6) was  
198 observed in lake 2 during a sunny day. Conductivity was below 100  $\mu\text{S cm}^{-1}$  in both lakes.  
199 The concentrations of dissolved inorganic nitrogen forms were low, whereas the  
200 concentration of dissolved reactive phosphorus (SRP) was 19.3  $\mu\text{g L}^{-1}$  in lake 2. Relatively  
201 high concentrations of dissolved organic carbon, particulate nutrients and chlorophyll-a were  
202 also characteristic for lake 2 (Table 1). Low autotrophic biomass in open water was mostly  
203 formed by detached benthic species; no substantial phytoplankton neither floating mats  
204 occurred in the lakes. The comparison of the two sampling dates available for lake 1  
205 suggested high fluctuations of dissolved nutrient concentrations.

### 206 **3.2 Thermal regime**

207 Figure 3a shows the annual variation of daily mean water temperature in lake 1 and of daily  
208 mean air temperature in the Solorina Valley (locations of temperature sensors are marked in  
209 Figures 1 and 2). Lake 1 was frozen to the bottom from the end of March to the end of  
210 October or beginning of November. Air temperatures were frequently lower than water  
211 temperatures. Minimum daily mean temperatures on the bottom of the lake were about  $-12\text{ }^{\circ}\text{C}$   
212 and  $-10\text{ }^{\circ}\text{C}$  for 2009 and 2010, respectively. Minimum daily mean air temperatures in the  
213 same period were between  $-32\text{ }^{\circ}\text{C}$  and  $-25\text{ }^{\circ}\text{C}$ . Mean monthly water temperatures in the lake  
214 ranged from  $-10.4\text{ }^{\circ}\text{C}$  (August 2009) to  $5.8\text{ }^{\circ}\text{C}$  (February 2010), while monthly mean air  
215 temperatures were between  $-18.7\text{ }^{\circ}\text{C}$  to  $0.7\text{ }^{\circ}\text{C}$ . The differences were greater at the beginning  
216 of the winter season (June–July), due to a rapid drop of air temperature.



217 The highest night-day air temperature fluctuations (up to 28 °C) were recorded during the  
218 winter months, while the lowest occurred in summer. In contrast, the highest night-day  
219 amplitudes of lake water temperature were recorded from November to February, with typical  
220 values between 2 °C and 4 °C (Figure 3b).

221 The course of global solar radiation (Figure 3c) was smooth, with the maximum daily mean of  
222 385 W m<sup>-2</sup> during clear sky conditions around the summer solstice. Global radiation reached  
223 the bottom of both lakes during the ice free period.

224 The relative frequency of hourly values of lake 1 water and air temperature is shown in Figure  
225 S1. Water temperature fluctuation was narrow, ranging from -16 to 8 °C. The bottom of the  
226 lake was frozen for most of the year, and the growing season, with water at temperatures from  
227 2 to 8 °C, covered only two-three months (Figure S1a). In contrast to lake water thermal  
228 regime, air temperature fluctuations were much wider (from -38 °C to 8 °C) (Figure S1b).

229 The temperature at the lake bottom was permanently below -4 °C only during the coldest  
230 two-three months per year (Fig. S2). The water temperature above 0 °C (liquid phase) was  
231 recorded from November to April (139 days in average). The number of days with  
232 temperature between 0 and -4 °C remains the same as for liquid water occurrence with small  
233 changes in the start and end dates towards to the transition period (February-June and  
234 September-November, respectively). In such thermal conditions, the benthic littoral  
235 community can be metabolically active.

### 236 **3.3 Littoral phyto­benthos – biofilm community description**

237 The littoral benthic community in lakes 1 and 2 are dominated by the heterocytous  
238 cyanobacterium *Calothrix elsteri* Komárek 2011 (Figure 4a), which forms a flat black biofilm  
239 on the upper surface of bottom stones (Figure 5), followed by *Hassallia andreassenni*  
240 Komárek 2011 and *Hassallia antarctica* Komárek 2011. *Hassallia andreassenni* is associated  
241 with calcium precipitation, as described later. *Hassallia antarctica* was found in stone  
242 crevices, being only loosely attached to the substrate. Littoral benthic mats – biofilms on  
243 stones (Figure 6) are co-dominated on the surface of the blackish cyanobacterial biofilm by  
244 the green filamentous and richly-branched alga *Hazenia broadyi* Škaloud et Komárek 2013  
245 (Ulotrichales, Chlorophyceae) (Figure 4b). *Hazenia broadyi* grew in macroscopic colonies  
246 producing green spots (Figure 5b,d). Later in the summer season, the green spots connected  
247 micro fortified mucilaginous lines (Figure 5c,d). Figure 5a shows the community in early  
248 spring whereas Figure 5b,d originated from later summer when the littoral benthic community

249 was already well developed with a dense coverage of *Hazenia broadyi* green spots. More  
250 detailed pictures (Figure 5e,f) documented the structure of the black leather like biofilm with  
251 mucilaginous marble on its surface covered by green spots. When the biofilm gets dry, the net  
252 of precipitated micro fortified mucilage mixed with [organic matter, mineral clasts](#) ~~soft mineral~~  
253 ~~matter~~ and crystals of calcium carbonate is visible (Figure 5g,h).

254 Scanning electron micrographs document the structure of the biofilm (Figure 7). Figure 7a  
255 shows a lateral view (cross section) of a biofilm with cyanobacterial filaments (*Calothrix*  
256 *elsteri* and *Hassallia andreassenni*). A biofilm upper view (Figure 7b,d) shows the structure  
257 of the cyanobacterial-microalgae community producing the mucilaginous micro fortified net  
258 of filaments with spots on its surface.

### 259 **3.4 Inorganic compounds of biofilms**

260 Thin sections, showing both dry biofilms and rock substrate (Figure 8), provided information  
261 on various inorganic compounds associated with the soft tissue of the cyanobacterial –  
262 microalgal community. These inorganic compounds are represented by (1) allochthonous  
263 mineral grains that are overgrown and incorporated by biofilms and (2) calcareous spicules of  
264 different sizes ranging from 0.5 mm to 1 cm that are precipitated within the cyanobacterial-  
265 microalgal community.

266 The rock substrate of biofilms is formed by subangular to subrounded pebbles to boulders of  
267 basaltic rock, which is dark-grey in colour, compact and usually with a microcrystalline  
268 porphyric texture. The rock is not homogenous, but contains numerous ball-like empty voids,  
269 which are often partly filled with feldspathoids (Figure 8a). Crystals of plagioclase (feldspar  
270 group) and augite (pyroxene group) are easily recognizable in thin sections (Figures 8a–c).

271 Biofilms are often partly covered with various mineral grains and rock fragments, but all  
272 specimens studied also contain these particles incorporated directly within soft cyanobacterial  
273 - microalgal [filaments-biofilm](#) (Figure 8a–c).

274 Mineral grains embedded within biofilms close to the basaltic rock surface are mainly angular  
275 to subangular crystal fragments of plagioclase and augite (Figures 8b,c), i.e. the main mineral  
276 components of the basaltic rock substrate described above. In the upper part of biofilms,  
277 however, partly or fully incorporated grains of quartz occur, being typically rounded or partly  
278 rounded (Figures 8a,b). One of the thin sections shows a calcareous spicule in situ and  
279 mineral grains within the biofilm (Figures 8c,d).

280 The structure and morphology of calcareous spicules was studied on SEM (Figure 9). ~~The~~  
281 ~~spicules (see also Methods) show an intensively worn surface (Figure 9a), partial or intense~~  
282 ~~recrystallization (Figures 9a,b) and dissolution (Figure 9b).~~ Crystal facets on the surface and  
283 cleavage (crystallographic structural planes) in the interior of the spicules (Figures 9a,b) are  
284 typical characteristics of calcium carbonate monocrystals.

285 ~~A non-recrystallized~~The superficial layer of microcrystalline calcite (e.g., Figure 9b) shows  
286 the structure of parallel needle-like calcite microcrystals (Figures 9d–f). Partial ~~corrosion and~~  
287 dissolution of spicules show distinct layering of these needle-like microcrystals (Figure 9d).  
288 The layered structure of ~~even partly recrystallized~~the spicules is confirmed in the ring-like  
289 structures with a possible cyanobacterial filament in the centre (Figure 10).

290 The chemical composition of the studied calcareous spicules determined by FSD corresponds  
291 to pure CaCO<sub>3</sub>. Following chemical composition, calcite and aragonite structural models were  
292 applied for the EBSD study focused on structural identification of the crystals forming the  
293 spicule. Structural identification of the studied specimen especially prepared for the EBSD  
294 study confirmed the absolute agreement between the recorded EBSD patterns and modelled  
295 patterns for calcite. The presence of aragonite was not confirmed. FSD images acquired for  
296 chemical and orientation contrasts (Figure 10) show a layered structure especially visible in  
297 orientation contrast. This feature reflects continual growing processes on layers with very  
298 similar crystallographic orientation. Absolute angular differences between individual layers  
299 are below 0.8°.

300

## 301 **4 Discussion**

### 302 **4.1 Environmental properties**

303 The lakes under study are characterized by a low content of major ions due to their volcanic  
304 bedrock and lower marine influence. In comparison with other lakes of this area, the two lakes  
305 show no specific lake water chemistry characteristics with moderate SRP and nitrate  
306 concentrations frequently below the detection limit (Nedbalová et al., 2013). High pH  
307 together with oxygen supersaturation recorded in lake 2 could be associated with high  
308 photosynthetic activity of the mats at the time of sampling.

309 Because water in either liquid or solid form has a large heat storage capacity, it acts as an  
310 important buffer to temperature change. Local climatic conditions of shallow freshwater lakes

311 is the principal external factor controlling their ecological functionality. Lake 1 is frozen to  
312 the bottom approximately eight-nine months per year. For most of the year, however, the  
313 temperature of the littoral and lake bottom is only from  $-2$  to  $-4$  °C. In such conditions, a thin  
314 layer of water probably covers the surface of the littoral benthic community that can be  
315 metabolically active (Davey et al., 1992). The growing season, with liquid water at  
316 temperatures between 2 to 4 °C, covers only two-three months.

317 In regards to heat balance, the studied shallow lakes are pond (wetlands) environments which  
318 freeze solid during the winter. This inevitability is a strong habitat-defining characteristic,  
319 which places considerable stress on resident organisms (Hawes et al., 1992; Elster, 2002). In  
320 summer, they must withstand drying in large parts of the littoral zone due to a considerable  
321 drop in water level. In freezing and desiccation resistance studies of freshwater phyto-benthos  
322 in shallow Antarctic lakes, several ecological measurements have recorded seasonal, diurnal,  
323 and year round temperature fluctuations and changes in water state transitions (e.g., Davey,  
324 1989; Hawes et al., 1992, Hawes et al., 1999). In localities with steady moisture and nutrient  
325 supplies, the abundance and species diversity of algae is relatively high. However, as the  
326 severity and instability of living conditions increases (mainly due to changes in mechanical  
327 disturbances, desiccation–rehydration and subsequent changes in salinity), algal abundance  
328 and species diversity decreases (Elster and Benson, 2004). The speed at which water state can  
329 change between liquid, ice, and complete dryness, is one of the most important ecological and  
330 physiological factors of these lakes. Studies based on field or laboratory experiments have  
331 shown that some cyanobacteria and algae are able to tolerate prolonged periods of desiccation  
332 (Pichrtová et al., 2014; Tashyreva and Elster, 2015). It is also obvious that there are  
333 strain/species specific differences in the overwintering strategies, and also between  
334 strains/species inhabiting different habitats (Davey, 1989; Hawes et al., 1992; Jacob et al.,  
335 1992; Šabacká and Elster, 2006; Elster et al., 2008). The ice and snow which cover the lakes  
336 for about eight-nine months per year serve as a natural incubator which moderate potential  
337 mechanical disturbances and stabilise the thermal regimes of the lakes.

## 338 **4.2 Biodiversity**

339 Patterns of endemism and alien establishment in Antarctica are very different across taxa and  
340 habitat types (terrestrial, freshwater or marine) (Barnes et al. 2006). Environmental  
341 conditions, as well as dispersal abilities, are important in limiting alien establishment (Barnes  
342 et al., 2006). Antarctic microbial (cyanobacteria, algae) diversity is still poorly known,

343 although recent molecular and ecophysiological evidence support a high level of endemism  
344 and speciation/taxon distinctness (Taton et al., 2003; Rybalka et al., 2009; de Wever et al.,  
345 2009; Komárek et al., 2011; Strunecký et al., 2012; Škaloud et al., 2013).

346 The floors of the studied lakes are covered with photosynthetic microbial mats composed of  
347 previously described species of heterocytous cyanobacteria, mostly *Calothrix elsteri* Komárek  
348 2011 followed by *Hassallia andreassenni* Komárek 2011 and *Hassallia antarctica* Komárek  
349 2011 (Komárek et al., 2011). They are co-dominated by a newly described species of green  
350 filamentous and richly branched algae *Hazenia broadyi* Škaloud et Komárek 2013  
351 (Ulotrichales, Chlorophyceae) (Škaloud et al., 2013). All the previously mentioned recently  
352 described species have special taxonomic positions together with special ecology and are  
353 considered at present as Antarctic endemic species.

354 The black leather like biofilm with mucilaginous marble on its surface is covered by green  
355 spots. These macroscopic structures form mats a few mm thick consisting of the above  
356 mentioned species packed in mucilage glued together with fine material. The regular leather  
357 biofilm structure with distinct cyanobacterial-microalgal composition and incorporated  
358 mineral grains is to our knowledge unique. During the limnological survey of the whole Ulu  
359 Peninsula (Nedbalová et al., 2013), this specific biofilm structure was observed only in the  
360 two endorheic lakes, although lakes with very similar morphometric and chemical  
361 characteristics are found in the area. The mat structure is thus apparently tightly linked to the  
362 species composition (Andersen et al., 2011).

363 The low abundance of benthic diatoms in the lakes is unusual, but not unprecedented as there  
364 are other areas in Antarctica where diatoms are scarce or absent (Broady, 1996, Wagner et al.,  
365 2004). The reason underlying the absence of diatoms is not immediately obvious, because  
366 diatoms are quite a common and frequently dominant component of microbial communities in  
367 most freshwater habitats of the Ulu Peninsula, James Ross Island (Kopalová et al., 2013).  
368 Local geographical separation of lakes 1 and 2 together with founder effect may have  
369 precluded successful colonization by the subset of diatoms that are common in the  
370 surrounding freshwater habitats. Although it has long been held that diatoms are dispersed  
371 widely, some recent reports document very small scale microbial distributions and endemism  
372 (Kopalová et al., 2012; Kopalová et al., 2013).

### 373 **4.3 Inorganic compounds of biofilms**

374 Based on the character of the rock substrate and lake sediments it is suggested, that one of the  
375 main prerequisites for existence of this cyanobacterial-microalgal community producing  
376 unusual biogenic calcite structures is; (1) flat and stable substrate in both lakes and (2) low  
377 sedimentation rate.

378 The substrate for biofilms is composed of boulders and pebbles of the stony littoral zone,  
379 petrographically corresponding to compact and massive basaltoids (Smellie et al., 2008;  
380 Svojtka et al., 2009). Rounded or sub-rounded quartz grains that are incorporated ("trapped")  
381 within biofilms cannot originate from basaltic volcanic rocks forming the bottom of both  
382 lakes and substrate of the studied biofilms. This is evidenced by the petrographic character of  
383 the basaltoids, which do not contain any quartz. The presence of abraded quartz grains in lake  
384 1 and 2 can be easily explained by wind transport (e.g., Shao, 2008).

385 The specific cyanobacterial-microalgal community described above can prosper in the two  
386 shallow endorheic lakes, because of low sedimentation rates resulting from minor water input.  
387 Low sedimentary input is the main necessary ecological parameter which facilitates the  
388 existence of this special microbial community. The community is, however, well adapted to  
389 seasonally elevated sedimentation rates coming from frequent and intense winds. During wind  
390 storms, the wind is carrying a relatively large amount of small mineral grains and rock  
391 microfragments (intense eolic erosion; e.g., Shao (2008) and references therein). These grains  
392 and particles are usually derived from erosion of the rocks either in the very close vicinity of  
393 the locality (weathering of basaltic rocks), but mainly come from remote locations where  
394 especially Upper Cretaceous marine sedimentary sequences are outcropping (Smellie et al.,  
395 | 2008; Svojtka et al., 2009). ~~Even elevated~~The amounts of mineral grains transported into the  
396 lake by wind do not stop the growth of cyanobacterial-microalgae biofilms, due to their ability  
397 of incorporating and "trapping" mineral grains within the living tissue (Riding, 2011).

398 This study has shown that inorganic substances precipitated by microbial lithogenetic  
399 processes are exclusively represented by calcite spicules. Precipitation of carbonate outside of  
400 microorganisms during photosynthesis as a mechanism of carbonate construction was  
401 described for many filamentous cyanobacterial species (Schneider and Le Campion-  
402 Alsumard, 1999). However, the biogenic calcite structures in both lakes are quite different to  
403 any microbially mediated structures yet described from modern environments (Kremer et al.,  
404 2008; Couradeau et al., 2011) and also to structures formed by abiotic precipitation (e.g., Vogt  
405 and Corte, 1996). Although there are many lakes with thick mats and similar chemical

406 characteristics on the Ulu Peninsula, the calcite spicules were found exclusively in the two  
407 endorheic lakes. We believe that their formation is linked to the specific photoautotrophic  
408 mats present in the lakes. From Figures 6g,h it is clearly visible that the calcareous  
409 organosedimentary structures keep contours of viable photosynthetic microbial mat after  
410 desiccation or calcite spicules precipitation. More specifically, the co-dominance of a green  
411 microalga is unique since mats in Antarctic lakes are most frequently formed by filamentous  
412 cyanobacteria (Vincent and Laybourn-Parry 2008). Therefore, we hypothesise that the more  
413 rapid photosynthesis rate of *Hazenia* in comparison with cyanobacteria may induce conditions  
414 necessary for carbonate precipitation in the lakes (Schneider and Le Campion-Alsumard,  
415 1999; Vincent, 2000). However, some role of abiotic precipitation of calcite is also possible.  
416 From our observations we cannot clearly decide if the winter abiotic calcite precipitation  
417 accompany microbial lithogenetic processes.

418 Although we interpret the tubular hollow observed in the centre of some spicules as the result  
419 of the presence of cyanobacterial filament during the process of crystallization, such  
420 structures may form also as the result of abiotic precipitation of calcite (Vogt and Corte, 1996;  
421 Fan and Wang, 2005).

422 It is striking that some calcite spicules probably exhibit recrystallization, forming spicules  
423 with the structure of calcite monocrystals. However, these spicules could be also interpreted  
424 as primary structures: mesostructured carbonate crystals formed through highly oriented  
425 growth of micro/nanocrystals and characterized by a specific surface texture (Fig. 9a–b).  
426 There is already evidence that some biominerals including calcite are mesocrystals (Cölfen  
427 and Antonietti, 2005) and the importance of extracellular polymeric substances for the  
428 formation of some types of [nanostructured](#) carbonate precipitates was documented (Pedley et  
429 al., 2009).

430 Determining the structure and material of precipitated inorganic substances brought another  
431 relevant question: "Do calcite spicules have fossilisation potential"? Microcrystalline calcite  
432 forming the recrystallized spicule is a typical material of calcite shells of fossil invertebrates  
433 (e.g., Vodrážka, 2009). Although calcite fossils may be partly or completely dissolved during  
434 diagenetical processes in the fossil record (e.g., Schneider et al., 2011; Švábenická et al.,  
435 2012), their preservation potential is relatively high. Therefore, we expect to find fossil and/or  
436 sub-fossil calcite spicules from the Quaternary lake sediments of the studied area.

437

## 438 **Acknowledgements**

439 This study was conducted during two Czech Antarctic research expeditions of the authors  
440 (J.E., L.N., R.V., K.L., J.K.) to the J. G. Mendel station in 2008 and 2009 (headed by Prof.  
441 Miloš Barták). We are indebted particularly to the staff and scientific infrastructure of the  
442 station. The study was supported by the Ministry of Education, Youth and Sports of the Czech  
443 Republic (CzechPolar LM2010009, [KONTAKT ME 945](#) and RVO67985939). R.V. has been  
444 funded through a Research and Development Project of the Ministry of Environment of the  
445 Czech Republic No. SPII 1a9/23/07 and [project GAČR GP14-31662P](#)~~by a project of the~~  
446 ~~Czech Geological Survey No. 338900~~. K.L. was supported by a project of Masaryk University  
447 MUNI/A/~~09021370/20142~~ “Global environmental changes ~~and their impacts in time and~~  
448 ~~space~~” ~~(Globe)~~. [The authors gratefully acknowledge the comments received from Kevin](#)  
449 [Lepot and two anonymous reviewers.](#) The technical work in laboratories was performed by  
450 Jana Šnokhousová and Dana Švehlová.

451

## 452 **References**

453 Andersen, D. T., Sumner, D. Y., Hawes, I., Webster-Brown, J., and McKay, C. P.: Discovery  
454 of large conical stromatolites in Lake Untersee, Antarctica. *Geobiology*, 9, 280–293, doi:  
455 10.1111/j.1472-4669.2011.00279.x, 2011.

456 Arp, G., Reimer, A., and Reitner, J.: Photosynthesis-induced biofilm calcification and calcium  
457 concentrations in Phanerozoic oceans. *Science*, 392, 1701, doi: 10.1126/science.1057204,  
458 2001.

459 Barnes, D. K. A., Hodgson, D. A., Convey, P., Allen, C. S., and Clarke, A.: Incursion and  
460 excursion of Antarctic biota: past, present and future. *Global Ecol. Biogeogr.*, 15, 121–142,  
461 doi: 10.1111/j.1466-822x.2006.00216.x, 2006.

462 Broady, P. A.: Diversity, distribution and dispersal of Antarctic terrestrial algae. *Biodiv.*  
463 *Conserv.*, 5, 1307–1335, doi: 10.1007/BF00051981, 1996.

464 Caspi, E. N., Pokroy, B., Lee, P. L., Quintana, J. P., and Zolotoyabko, E.: On the structure of  
465 aragonite. *Acta Crystallogr.*, B 61, 129–132, doi: 10.1107/S0108768105005240, 2005.



466 Clark, I. D. and Lauriol, B.: Aufeis of the Firth River basin, Northern Yukon Canada: insights  
467 to permafrost hydrology and karst. *Arct. Alp. Res.*, 29, 240–252, doi: 10.2307/1552053, 1997.

468 Courty, M. A., Marlin, C., Dever, L., Tremblay, P., and Vachier, P.: The properties, genesis  
469 and environmental significance of calcite pendants from the high Arctic (Spitsbergen).  
470 *Geoderma*, 61, 71–102, doi: 10.1016/0016-7061(94)90012-4, 1994.

471 Couradeau, E., Benzerara, K., Moreira, D., Gérard, E., Kaźmierczak, J., Tavera, R. and  
472 López-García, P.: Prokaryotic and eukaryotic community structure in field and cultured  
473 microbialites from the alkaline lake Alchichica (Mexico). *PloS ONE*, 6, 1–15, doi:  
474 10.1371/journal.pone.0028767, 2011.

475 Cölfen, H. and Antonietti, M.: Crystal design of calcium carbonate microparticles using  
476 double-hydrophilic block copolymers. *Langmuir*, 14, 582–589, doi: 10.1021/la970765t, 1998.

477 Cölfen, H. and Antonietti, M.: Mesocrystals: inorganic superstructures made by highly  
478 parallel crystallization and controlled alignment. *Angew. Chem. Int. Ed.*, 44, 5576–5591, doi:  
479 10.1002/anie.200500496, 2005.

480 Davies, B. J., Glasser, N.F., Carrivick, J. L., Hambrey, M. J., Smellie, J. L., and Nývlt, D.:  
481 Landscape evolution and ice-sheet behavior in a semi-arid polar environment: James Ross  
482 Island, NE Antarctic Peninsula. Special publication. Geological Society of London, doi:  
483 10.1144/SP381.1, 2013.

484 Davey, M. C.: The effect of freezing and desiccation on photosynthesis and survival of  
485 terrestrial Antarctic algae and cyanobacteria. *Polar Biol.*, 10, 29–36, 1989.

486 Davey, M. C., Pickup, J., and Block, W.: Temperature variation and its biological  
487 significance in fellfield habitats on a maritime Antarctic island. *Antarct Sci.*, 4, 383–388,  
488 1992.

489 De Wever, A., Leliaert, F., Verleyen, E., Vanormelingen, P., Van der Gucht, K., Hodgson, D.  
490 A., Sabbe, K., and Vyverman, W.: Hidden levels of phylodiversity in Antarctic green algae:  
491 further evidence for the existence of glacial refuge. *P. Roy. Soc. B-Biol. Sci.*, 276, 3591–  
492 3599, doi: 10.1098/rspb.2009.0994, 2009.

493 Effenberger, H., Mereiter, K., and Zemann, J.: Crystal structure refinements of magnesite,  
494 calcite, rhodochrosite, siderite, smithsonite and dolomite, with discussion of some aspects of  
495 the stereochemistry of calcite-type carbonates. *Z. Kristallogr.*, 156, 233–243, 1981.

496 Elster, J.: Ecological classification of terrestrial algal communities of polar environment, in:  
497 *GeoEcology of terrestrial oases*, edited by: Beyer, L. and Boelter, M., 303–319. *Ecological*  
498 *Studies*, Springer-Verlag, Berlin, Heidelberg, 2002.

499 Elster, J. and Benson, E. E.: Life in the polar terrestrial environment with a focus on algae and  
500 cyanobacteria, in: *Life in the frozen state*, edited by: Fuller, B., Lane, N. and Benson E. E.,  
501 111–149. Taylor and Francis, London, doi: 10.1201/9780203647073.ch3, 2004.

502 Elster, J., Degma, P., Kováčik, L., Valentová, L., Šrámková, K., and Pereira, A. B.: Freezing  
503 and desiccation injury resistance in the filamentous green alga *Klebsormidium* from the  
504 Antarctic, Arctic and Slovakia. *Biologia*, 63, 839–847, doi: 10.2478/s11756-008-0111-2,  
505 2008.

506 Fairchild, I. J., Bradby, B., and Spiro, B.: Carbonate diagenesis in ice. *Geology*, 21, 901–904,  
507 doi: 10.1130/0091-7613(1993)021<0901:CDII>2.3.CO;2, 1993.

508 Fan, Y.W. and Wang, R.Z.: Submicrometer-sized vaterite tubes formed through nanobubble-  
509 templated crystal growth. *Adv. Mater.*, 17, 2384–2388, doi: 10.1002/adma.200500755, 2005.

510 Jacob, A., Wiencke, C., Lehmann, H., and Krist, G. O.: Physiology and ultrastructure of  
511 desiccation in the green alga *Prasiola crispa* from Antarctica. *Bot. Mar.*, 35, 297–303, doi:  
512 10.1515/botm.1992.35.4.297, 1992.

513 Johnson, J. S., Bentley, M. J., Roberts, S. J., Binnie, S. A., and Freeman, S. P. H. T.:  
514 Holocene deglacial history of the northeast Antarctic Peninsula – A review and new  
515 chronological constraints. *Quaternary Sci. Rev.*, 30, 3791–3802, doi:  
516 10.1016/j.quascirev.2011.10.011, 2011.

517 Hawes, I., Smith, R., Howard-Williams, C., and Schwarz, A. M.: Environmental conditions  
518 during freezing, and response of microbial mats in ponds of the McMurdo Ice Shelf,  
519 Antarctica. *Antarct. Sci.*, 11, 198–208, 1999.

520 Hawes, I., Howard-Williams, C., and Vincent, W. F.: Desiccation and recovery of Antarctic  
521 cyanobacterial mats. *Polar Biol.*, 12, 587–594, 1992.

522 Hawes, I., Moorhead, D., Sutherland, D., Schmeling, J., and Schwarz, A. M.: Benthic primary  
523 production in two perennially ice-covered Antarctic lakes: pattern of biomass accumulation  
524 with a model of community metabolism. *Antarct.Sci.*, 13, 18–27, 2001.

525 Komárek, J. and Elster, J.: Ecological background of cyanobacterial assemblages of the  
526 northern part of James Ross Island, NW Weddell Sea, Antarctica. *Pol. Polar Res.*, 29, 17–32,  
527 2008.

528 Komárek, J., Nedbalová, L., and Hauer, T.: Phylogenetic position and taxonomy of three  
529 heterocytous cyanobacteria dominating the littoral of deglaciated lakes, James Ross Island,  
530 Antarctica. *Polar Biol.*, 35, 759–774, doi: 10.1007/s00300-011-1123-x, 2011.

531 Komárek, J., Bonaldo, G. D., Fatima, F. M., and Elster, J.: Heterocytous cyanobacteria of the  
532 Ulu Peninsula, James Ross Island, Antarctica. *Polar Biol.*, 38, 475–492, doi: 10.1007/s00300-  
533 014-1609-4, 2015.

534 Kopalová, K., Veselá, J., Elster, J., Nedbalová, L., Komárek, J., and Van de Vijver, B.:  
535 Benthic diatoms (Bacillariophyta) from seepages and streams on James Ross Island (NW  
536 Weddell Sea, Antarctica). *Plant Ecol. Evol.*, 145, 1–19, doi: 10.5091/plecevo.2012.639, 2012.

537 Kopalová, K., Nedbalová, L., Nývlt, D., Elster, J., and Van de Vijver, B.: Diversity, ecology  
538 and biogeography of the freshwater diatom communities from Ulu Peninsula (James Ross  
539 Island, NE Antarctic Peninsula). *Polar Biol.*, 36, 933–948, doi: 10.1007/s00300-013-1317-5,  
540 2013.

541 Kremer, B., Kaźmierczak, J., and Stal, L. J.: Calcium carbonate precipitation in cyanobacteria  
542 mats from sandy tidal flats of the North Sea. *Geobiology*, 6, 46–56, doi: 10.1111/j.1472-  
543 4669.2007.00128.x, 2008.

544 Láska, K., Barták, M., Hájek, J., Prošek, P., and Bohuslavová, O.: Climatic and ecological  
545 characteristics of deglaciated area of James Ross Island, Antarctica, with a special respect to  
546 vegetation cover. *Czech Polar Reports*, 1, 49–62, 2011a.

547 Láska, K., Budík, L., Budíková, M., and Prošek, P.: Method of estimating of solar UV  
548 radiation in high-latitude locations based on satellite ozone retrieval with improved algorithm.  
549 *Int. J. Remote Sens.*, 32, 3165–3177, doi: 10.1080/01431161.2010.541513, 2011b.

550 Lepot, K., Compère, P., Gérard, E., Namsaraev, Z., Verleyen, E., Tavernier, I., Hodgson, D.  
551 A., Vyverman, W., Gilbert, B., and Javaux, E. J. : Organic and mineral imprints in fossil  
552 photosynthetic mats of an East Antarctic lake. *Geobiology*, 12, 424–450, doi:  
553 10.1111/gbi.12096, 2014.

554 Nakai, N., Wada, H., Kiyoshu, Y., and Takimoto, M.: Stable isotope studies on the origin and  
555 geological history of water and salts in the Lake Vanda area, Antarctica. *Geochem. J.*, 9, 7–  
556 24, 1975.

557 Nedbalová, L., Nývlt, D., Kopáček, J., Šobr, M., and Elster, J.: Freshwater lakes of Ulu  
558 Peninsula, James Ross Island, north-east Antarctic Peninsula: origin, geomorphology, and  
559 physical and chemical limnology. *Antarct. Sci.*, 25, 358–372, doi:  
560 10.1017/S0954102012000934, 2013.

561 Ng, F. and Hallet, B.: Patterning mechanisms in subglacial carbonate dissolution and  
562 deposition. *J. Glaciol.*, 48, 386–400, 2002.

563 Nývlt, D., Košler, J., Mlčoch, B., Mixa, P., Lisá, L., Bubík, M., and Hendriks, B. W. H.: The  
564 Mendel Formation: evidence for late Miocene climatic cyclicity at the northern tip of the  
565 Antarctic Peninsula. *Palaeogeogr. Palaeoclimatol.*, 299, 363–394, 10.1016/j.palaeo.2010.11.017,  
566 2011.

567 Olivero, E. B., Scasso, R. A., and Rinaldi, C. A.: Revision of the Marambio Group, James  
568 Ross Island, Antarctica. Instituto Antartico Argentino, Contribución, 331, 1–28, 1986.

569 Øvstedal, D. O., and Lewis Smith, R. I.: Lichens of Antarctica and South Georgia: A guide to  
570 their identification and ecology. *Studies in Polar Research*, Cambridge University Press,  
571 Cambridge, 411 pp, 2001.

572 Pechar, L.: Use of acetone:methanol mixture for the extraction and spectrophotometric  
573 determination of chlorophyll a in phytoplankton. *Archiv für Hydrobiologie/Supplement*,  
574 *Algological Studies*, 46, 99–117, 1987.

575 Pedley, M., Rogerson, M., and Middleton, R.: Freshwater calcite precipitates from in vitro  
576 mesocosm flume experiments: a case for biomediation of tufas. *Sedimentology* 56, 511-527,  
577 doi: 10.1111/j.1365-3091.2008.00983.x, 2009.

578 Pichrtová, M., Hájek, T., and Elster, J.: Osmotic stress and recovery in field populations of  
579 *Zygnema* sp. (Zygnematophyceae, Streptophyta) on Svalbard (High Arctic) subjected to  
580 natural desiccation. *FEMS Microbiol. Ecol.*, 89, 270–280, doi:10.1111/1574-6941.12288,  
581 2014.

582 Rabassa, J., Skvarca, P., Bertani, L., and Mazzoni, E.: Glacier inventory of James Ross and  
583 Vega Islands, Antarctic Peninsula. *Ann. Glaciol.*, 3, 260–264, 1982.

584 Reid, P., Dupraz, C., Visscher, P., and Sumner, D.: Microbial processes forming marine  
585 stromatolites, in: *Fossil and recent biofilms – a natural history of life on Earth*, edited by:  
586 Krumbein, W.E., Peterson, D.M., and Zavarzin, G. A., 103–118. Kluwer Academic  
587 Publishers, London, 2003.

588 Riding, R.: Microbialities, stromatolites, and thrombolites, in: *Encyclopedia of Geobiology*,  
589 edited by: Reitner, J. and Thiel, V., 635–654, *Encyclopedia of Earth Science Series*, Springer,  
590 Heidelberg, 2011.

591 Rybalka, N., Andersen, R. A., Kostikov, I., Mohr, K. I., Massalski, A., Olech, M., and Friedl,  
592 T.: Testing for endemism, genotypic diversity and species concepts in Antarctic terrestrial  
593 microalgae of the Tribonemataceae (Stramenophiles, Xanthophyceae). *Environ. Microbiol.*,  
594 11, 554–565, doi: 10.1111/j.1462-2920.2008.01787.x, 2009.

595 Šabacká, M. and Elster, J.: Response of cyanobacteria and algae from Antarctic wetland  
596 habitats to freezing and desiccation stress. *Polar Biol.*, 30, 31–37, doi: 0.1007/s00300-006-  
597 0156-z, 2006.

598 Shao, Y.: *Physics and Modelling of Wind Erosion*. Atmospheric and Oceanographic  
599 Sciences Library 37. 2nd Edition. Springer, Heidelberg. 456 pp, 2008.

600 Schieber, J.: Microbial mats in terrigenous clastics: the challenge of identification in the rock  
601 record. *Palaios*, 14, 3–12, doi: 10.2307/3515357, 1999.

- 602 Schmidt, N. H. and Olesen, N. O.: Computer-aided determination of crystal-lattice  
603 orientation from electron-channeling patterns in the SEM. *Can. Mineral.*, 28, 15–22, 1989.
- 604 Schneider, S. and Le Campion-Alsumard, T.: Construction and destruction of carbonates by  
605 marine and freshwater cyanobacteria. *Eur. J. Phycol.*, 34, 417–426, doi:  
606 10.1017/S0967026299002280, 1999.
- 607 Schneider, J., Niebuhr, B., Wilmsen, M., and Vodrážka, R.: Between the Alb and the Alps –  
608 The fauna of the Upper Cretaceous Sandbach Formation (Passau region, southeast Germany).  
609 *Bull. Geosci.*, 86, 785–816, doi: 10.3140/bull.geosci.1279, 2011.
- 610 Škaloud, P., Nedbalová, L., Elster, J., and Komárek, J.: A curious occurrence of *Hazenia*  
611 *broadyi* spec. nova in Antarctica and the review of the genus *Hazenia* (Ulotrichales,  
612 Chlorophyceae). *Polar Biol.*, 36, 1281–1291, doi: 10.1007/s00300-013-1347-z, 2013.
- 613 Smellie, J. L., Johnson, J. S., McIntosh, W. C., Esser, R., Gudmundsson, M. T., Hambrey, M.  
614 J., and Van Wyk de Vries, B.: Six million years of glacial history recorded in volcanic  
615 lithofacies of the James Ross Island Volcanic Group, Antarctic Peninsula. *Palaeogeogr.*  
616 *Palaeocl.*, 260, 122–148, doi: 10.1016/j.palaeo.2007.08.011, 2008.
- 617 Strunecký, O., Elster, J., and Komárek, J.: Molecular clock evidence for survival of Antarctic  
618 cyanobacteria (*Oscillatoriales*, *Phormidium autumnale*) from Paleozoic times. *FEMS*  
619 *Microbiol. Ecol.*, 82, 482–490, doi: 10.1111/j.1574-6941.2012.01426.x, 2012.
- 620 Sutherland, D. and Hawes, I.: Annual growth layers as proxies for past growth conditions for  
621 benthic microbial mats in a perennially ice-covered Antarctic lake. *FEMS Microbiol. Ecol.*, 67,  
622 279–292, doi: 10.1111/j.1574-6941.2008.00621.x, 2009.
- 623 Švábenická, L., Vodrážka, R., and Nývlt, D.: Calcareous nanofossils from the Upper  
624 Cretaceous of northern James Ross Island, Antarctica. *Geol. Q.*, 56, 765–772, doi:  
625 10.7306/gq.1053, 2012.
- 626 Svojtka, M., Nývlt, D., Muramaki, M., Vávrová, J., Filip, J., and Mixa, P.: Provenance and  
627 post-depositional low-temperature evolution of the James Ross Basin sedimentary rocks  
628 (Antarctic Peninsula) based on fission track analysis. *Antarct. Sci.*, 21, 593–607, doi:  
629 10.1017/S0954102009990241, 2009.

630 Tashyreva, D. and Elster, J.: The limits of desiccation tolerance of Arctic *Microcoleus* strains  
631 (Cyanobacteria) and environmental factors inducing desiccation tolerance. *Front. Microbiol.*,  
632 doi: 10.3389/fmicb.2015.00278, 2015.

633 Taton, A., Grubisic, S., Brambilla, E., de Wit, R., and Wilmotte, A.: Cyanobacterial diversity  
634 in natural and artificial microbial mats of Lake Fryxell (McMurdo Dry Valleys, Antarctica): a  
635 morphological and molecular approach. *Appl. Environ. Microb.*, 69, 5157–5169, doi:  
636 10.1128/AEM.69.9.5157-5169.2003, 2003.

637 Turner, J., Barrand, N. E., Bracegirdle, T. J., Convey, P., Hodgson, D. A., Jarvis, M., Jenkins,  
638 A., Marshall, G., Meredith, M. P., Roscoe, H., Shanklin, J., French, J., Goose, H.,  
639 Guglielmin, M., Gutt, J., Jacobs, S., Kennicutt, M. C., Valerie Masson-Delmotte, II.,  
640 Mayewski, P., Navarro, F., Robinson, S., Scambos, T., Sparrow, M., Summerhayes, C.,  
641 Speer, K., and Klepikov, A.: Antarctic climate change and the environment: an update. *Polar*  
642 *Rec.*, 50, 237–259, doi: 10.1017/S0032247413000296, 2014.

643 Vincent, W. F. and Laybourn-Parry, J. (Eds.): *Polar lakes and rivers*. Oxford University Press,  
644 Oxford, 346 pp, doi: 10.1093/acprof:oso/9780199213887.001.0001, 2008.

645 Vincent, W. F.: Cyanobacterial dominance in polar regions, in: *The Ecology of*  
646 *Cyanobacteria*, edited by: Whitton B. A. and Potts, M., 321–340. Kluwer Academic  
647 Publishers, the Netherlands, 2000.

648 Vodrážka, R.: A new method for the extraction of microfossils from calcareous rocks using  
649 sulphuric acid. *Palaeontology*, 52, 187–192, doi: 10.1111/j.1475-4983.2008.00829.x, 2009.

650 Vogt, T. and Corte, A. E.: Secondary precipitates in Pleistocene and present cryogenic  
651 environments (Mendoza Precordillera, Argentina, Transbaikalia, Siberia, and Seymour Island  
652 Antarctica). *Sedimentology*, 43, 53–64, doi: 10.1111/j.1365-3091.1996.tb01459.x, 1996.

653 Wadham, J. L., Tranter, M., and Dowdeswell, J. A.: Hydrochemistry of meltwaters draining a  
654 polythermal-based, high-Arctic glacier, south Svalbard: II. Winter and early spring. *Hydrol.*  
655 *Process.*, 14, 1767–1786, doi: 10.1002/1099-1085(200007)14:10<1767: AID-  
656 HYP103>3.0.CO;2-Q, 2000.

657 Wagner, B., Cremer, H., Hulzsch, N., Gore, D., and Melles, M.: Late Pleistocene and  
658 Holocene history of Lake Terrasovoje, Amery Oasis, East Antarctica, and its climatic and  
659 environmental implications. *J. Paleolimnol.*, 32, 321–339, doi: 10.1007/s10933-004-0143-8,  
660 2004.

661 Walter, M.: *Stromatolites*. Elsevier Science Ltd., Amsterdam, the Netherlands, 1976, 790 pp.

662 Wharton, R. A., Parker, B. C., Simmons, G. M., and Love, F. G.: Biogenic calcite structures  
663 forming in Lake Fryxell, Antarctica. *Nature*, 295, 403–405, doi: 10.1038/295403a0, 1982.

664 Wharton, R.: Stromatolitic mats in Antarctic lakes, in: *Phanerozoic Stromatolites, II*, edited  
665 by: Bertrand-Safari, J. and Monty, C., 53–70, Springer, New York, USA, doi: 10.1007/978-  
666 94-011-1124-9\_3, 1994.

667 Yamamoto, A., Tanabe, K., and Isozaki, Y.: Lower Cretaceous freshwater stromatolites from  
668 northern Kyushu, Japan. *Paleontol. Res.*, 13, 139–149, 10.2517/1342-8144-13.2.139, 2009.

669

670

671

672

673

674

675

676

677

678

679

680

681

682

683

684

685



686 Table 1. Physico-chemical characteristics and chlorophyll-a concentrations in lake water.  
 687 Samples were collected from surface of lakes. ND – not determined, ANC – acid  
 688 neutralization capacity, PN – particulate nitrogen, DP – dissolved phosphorus, PP –  
 689 particulate phosphorus, SRP – dissolved reactive phosphorus, DOC – dissolved organic  
 690 carbon, PC – particulate carbon, \* – laboratory values.

Lake		Green 1	Green 2	
Date		22.2.2008	5.1.2009	12.1.2009
Temperature	°C	3.5	ND	12.3
O <sub>2</sub>	mg L <sup>-1</sup>	13.1	ND	13.7
O <sub>2</sub> saturation	%	98.7	ND	128.0
pH		7.9	7.4*	8.6
Conductivity (25 °C)	µS cm <sup>-1</sup>	54	48*	97
ANC	mmol L <sup>-1</sup>	236	246	455
Na <sup>+</sup>	mg L <sup>-1</sup>	4.7	5.9	12.5
K <sup>+</sup>	mg L <sup>-1</sup>	0.24	0.29	0.60
Ca <sup>2+</sup>	mg L <sup>-1</sup>	2.12	1.26	2.32
Mg <sup>2+</sup>	mg L <sup>-1</sup>	1.24	0.77	1.65
SO <sub>4</sub> <sup>2-</sup>	mg L <sup>-1</sup>	1.74	1.33	2.60
Cl <sup>-</sup>	mg L <sup>-1</sup>	5.3	5.1	10.6
NO <sub>3</sub> -N	µg L <sup>-1</sup>	<5	11	<5
NO <sub>2</sub> -N	µg L <sup>-1</sup>	0.6	0.2	0.1
NH <sub>4</sub> -N	µg L <sup>-1</sup>	6	<5	<5
PN	µg L <sup>-1</sup>	20	50	73
DP	µg L <sup>-1</sup>	7.8	20.2	30.4
PP	µg L <sup>-1</sup>	4.6	5.9	11.7
SRP	µg L <sup>-1</sup>	4.0	11.6	19.3
DOC	mg L <sup>-1</sup>	1.25	1.13	2.17
PC	mg L <sup>-1</sup>	0.13	0.41	1.33
Si	mg L <sup>-1</sup>	1.45	0.87	2.85
chl- <i>a</i>	µg L <sup>-1</sup>	0.9	ND	6.0

691

692

693 **Figure captions**

694 Figure 1. Location of lake 1 and 2 and air temperature measurements (ASW) in the Solorina  
695 Valley.

696

697 Figure 2. Bathymetric parameters of lake 1 (a) and 2 (b) together with marked lines of water  
698 level and maximum extent of the photosynthetic microbial mat littoral belt in lake 1.

699

700 Figure 3. a – annual variation of daily mean water temperature in lake 1 (L1 water) and annual  
701 variation of daily mean air temperature in the Solorina Valley (SV air), b – diurnal  
702 temperature amplitudes in lake 1 (L1 water) and diurnal air temperature amplitudes in the  
703 Solorina Valley (SV air), respectively. c – daily mean global radiation at Mendel Station. All  
704 parameters measured from February 2009 to November 2010.

705

706 Figure 4. Dominant species in the photoautotrophic mats.

707 a – *Calothrix elsteri*,

708 b – *Hazenia broadyi*

709

710 Figure 5. Photoautotrophic mats in lakes 1 and 2.

711 a,b – rapid development of the mat in January 2009 (lake 1). The two photos show the mat at  
712 a one week interval, note the growth of gelatinous clusters of densely agglomerated filaments  
713 of the green alga *Hazenia broadyi*,

714 c,d – fully developed mats with mosaic-like structures on the surfaces of stones in the littoral  
715 zone of lake 2,

716 e,f – detail,

717 g – drying of the mat in the littoral zone leaves a characteristic structure on the surface of  
718 stones,

719 h – calcium carbonate spicule in situ (arrowed)

720

721 Figure 6. Photoautotrophic mat covering a stone visualized using imaging fluorometry.

722 a – upper view,

723 b – lateral view

724

725 Figure 7. SEM macrographs showing the structure of the dried mat in the lakes.

726 a – transversal section of the mat with visible cyanobacterial filaments,

727 b – surface structure of the mat, the position of cyanobacterial filaments incorporated within  
728 mucilaginous matrix is indicated by arrows,

729 c – general view of the surface structure of the mat with the net formed by mucilage (compare  
730 with Fig. 7d),

731 d – detail of the same mucilaginous structure

732

733 Figure 8. Perpendicular thin sections of rock substrate covered by dry biofilms (recorded  
734 under cross polars). Note that biofilms are partly detached from the surface of the rock due to  
735 complete drying of the sample.

736 a – conspicuous U-shaped empty void (arrowed "2") near the surface of basaltic rock partly  
737 infilled with crystals of feldspathoids (tectosilicate minerals, arrowed "1"); empty void is  
738 bridged by biofilm (arrowed "3") with partly incorporated mineral clasts, represented by semi-  
739 rounded quartz grains (arrowed "4"),

740 b – rather thick biofilm with numerous incorporated mineral grains. Note that close to the  
741 rock substrate the angular grains of plagioclase (feldspar group) and augite (pyroxene group)  
742 dominate, being derived from basaltoids, whereas close to the surface rounded grains of  
743 quartz occur (arrowed),

744 c – in situ calcium carbonate spicule penetrating biofilm and surrounded by incorporated  
745 grains of feldspars (two arrows on the left) and pyroxene (arrow on the right),

746 | d – close up of the same calcium carbonate spicule with [aa possible](#) cyanobacterial filament in  
747 its centre

748

749 | Figure 9. SEM macrographs showing the morphology of ~~partly recrystallized~~ calcium  
750 | carbonate spicules. Spicules were washed away from the living tissue and collected directly  
751 | from the surface of biofilms, although residence time on the bottom cannot be determined.

752 | a – calcareous spicule showing specific surface texture (“worn surface”) ~~and complete~~  
753 | ~~recrystallization of the spicule interior~~. The spicule shows crystal facets on the surface and  
754 | cleavage (crystallographic structural planes) in the interior (arrowed) – i.e. typical  
755 | characteristics of calcium carbonate monocrystal,

756 | b – detail of previous image; two parallel systems of deep furrows on the surface are  
757 | crystallographic structural planes of calcite monocrystal; remnants of a superficial layer of  
758 | microcrystalline calcite are, however, preserved in places on the surface of the crystal  
759 | (arrowed),

760 | c-f – ~~poorly recrystallized~~ ~~another type of~~ spicule, formed mainly by microcrystalline calcite,

761 | c – lateral view of the spicule,

762 | d – detail of the surface showing ~~corrosion of~~ needle-like calcite microcrystals with distinct  
763 | layering,

764 | e – parallel needle-like calcite microcrystals on the surface of the central part of the spicule,

765 | f – tops of parallel needle-like calcite microcrystals on the surface of the terminal part of the  
766 | spicule; the view is perpendicular with respect to the previous macrograph

767

768 | Figure 10. FSD image of a transversely sectioned, partly recrystallized calcite spicule  
769 | acquired in (a) chemical contrast, (b) orientation contrast

770

771

772

773

774

775

776

777

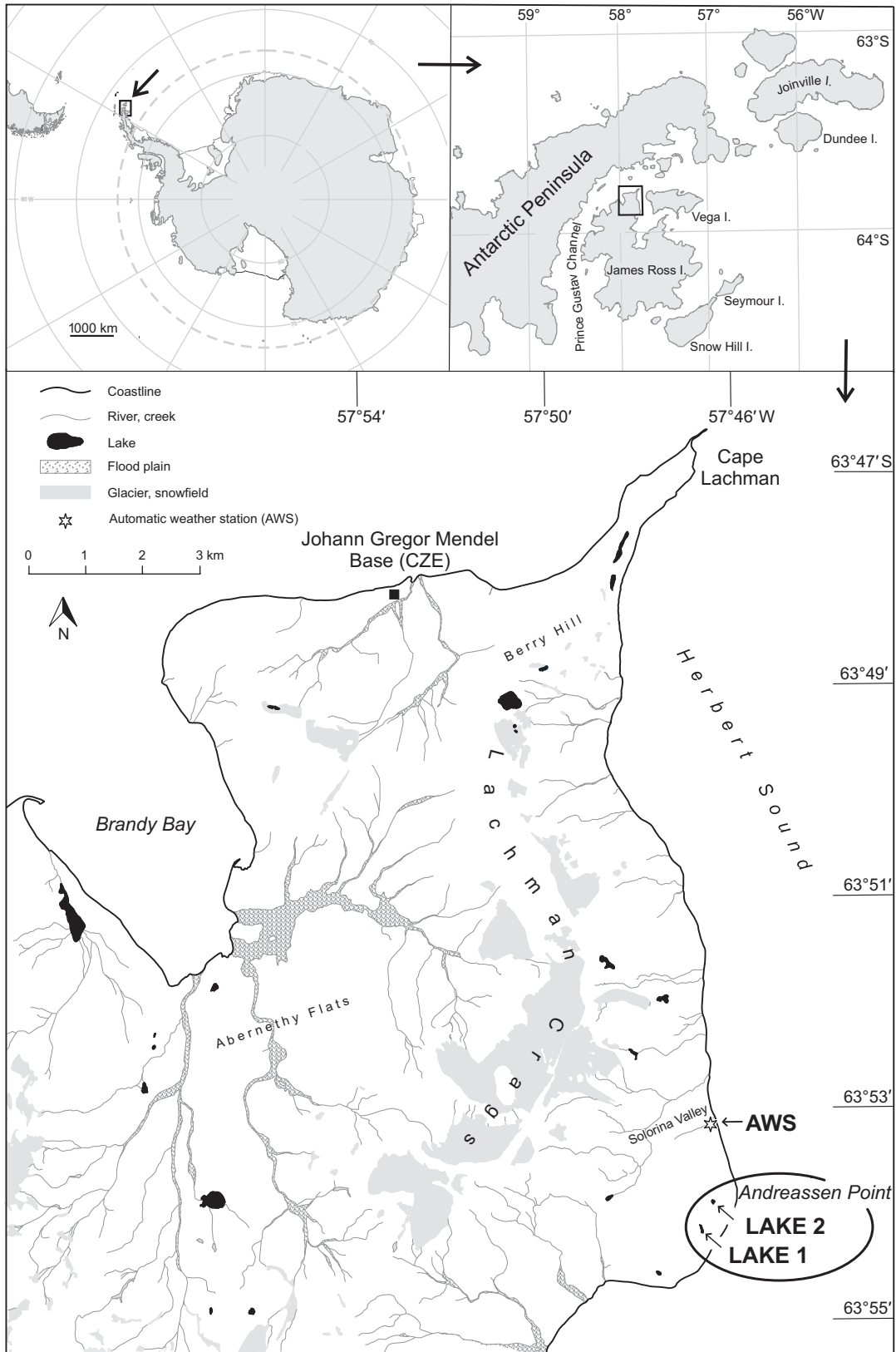


Fig. 1

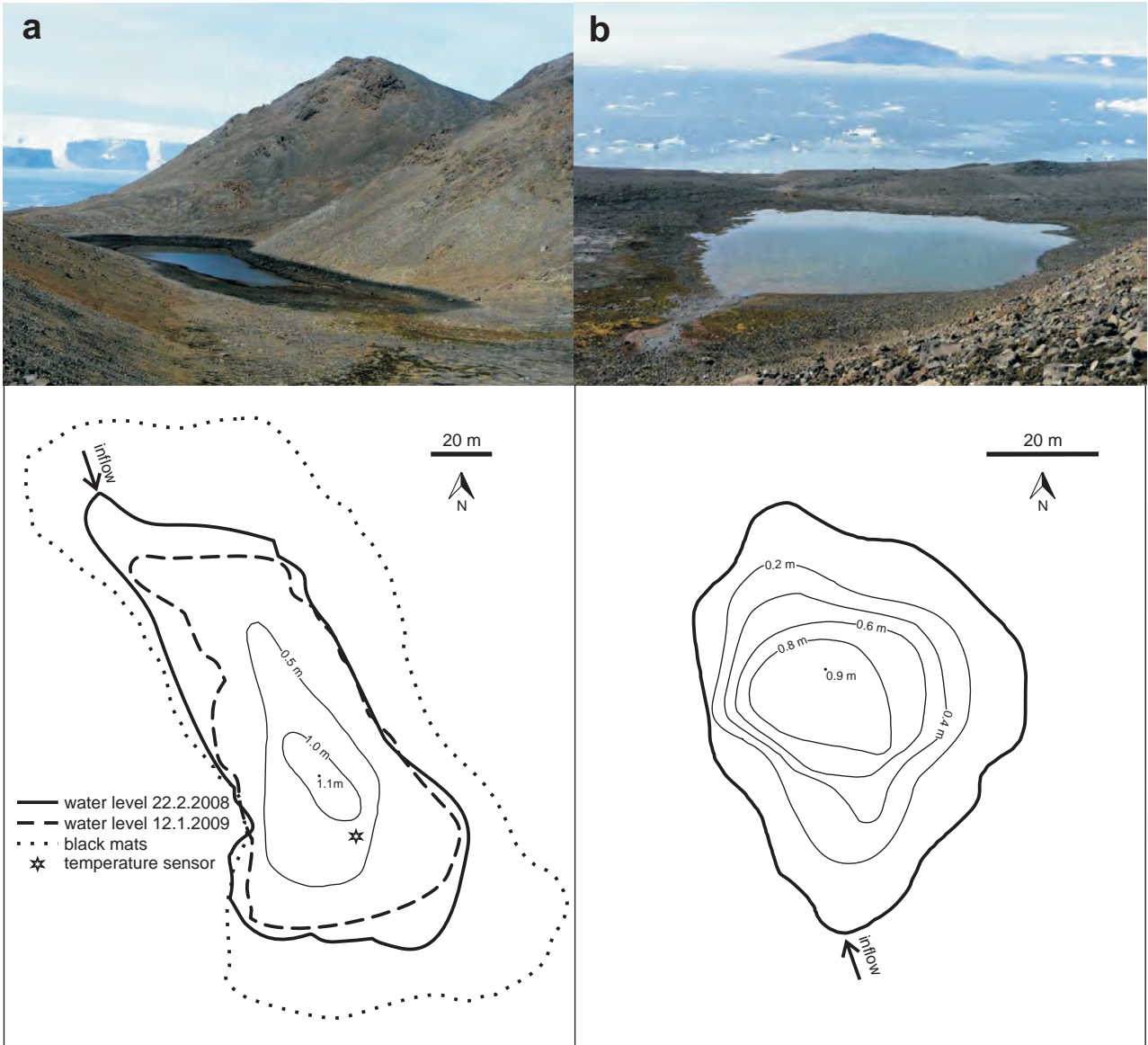


Fig. 2

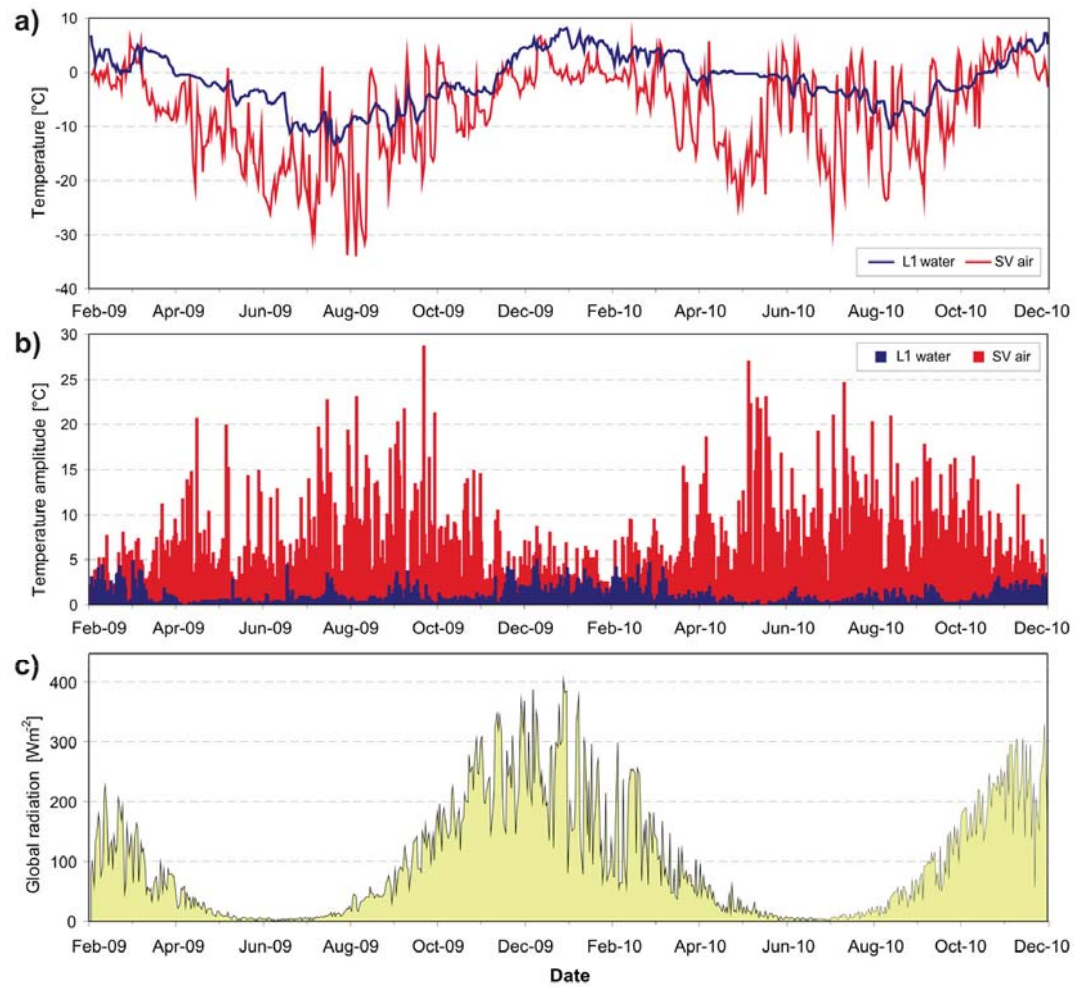


Fig. 3

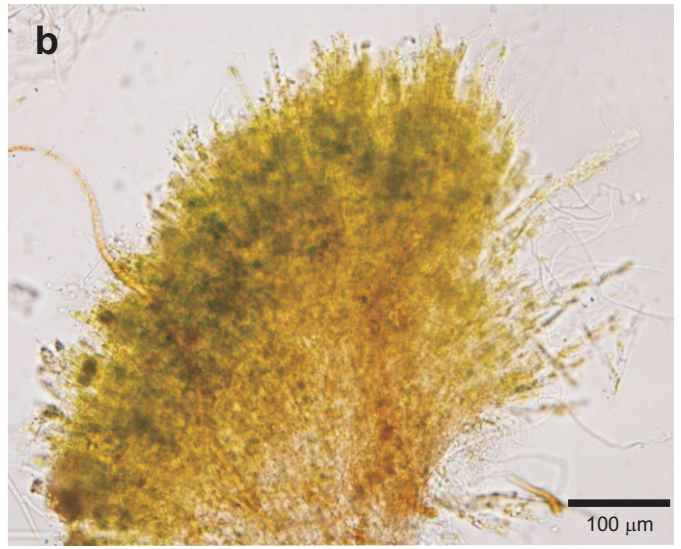
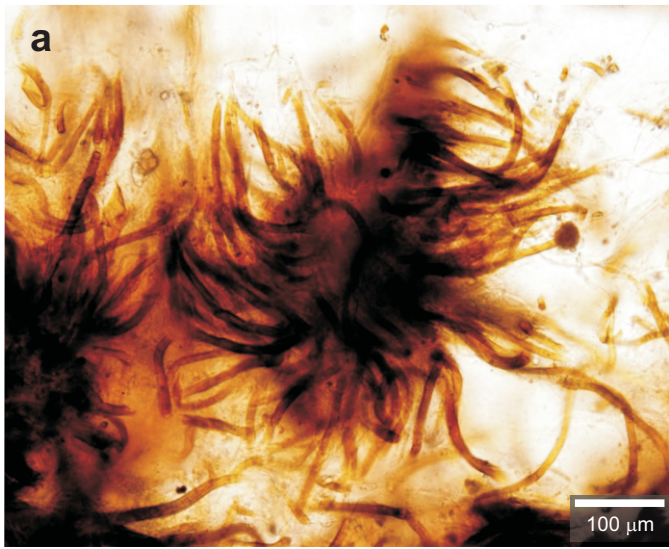


Fig. 4



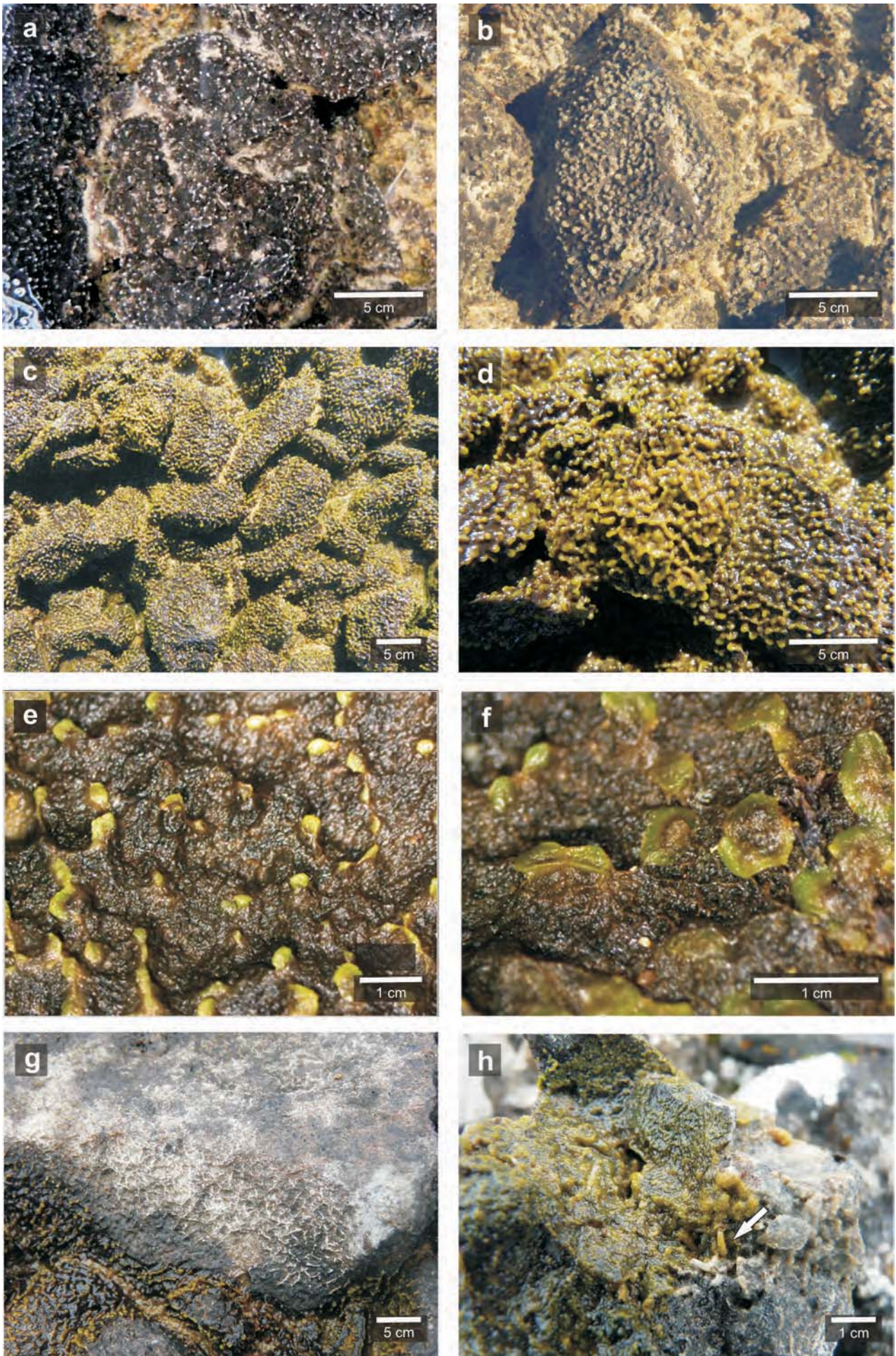


Fig. 5

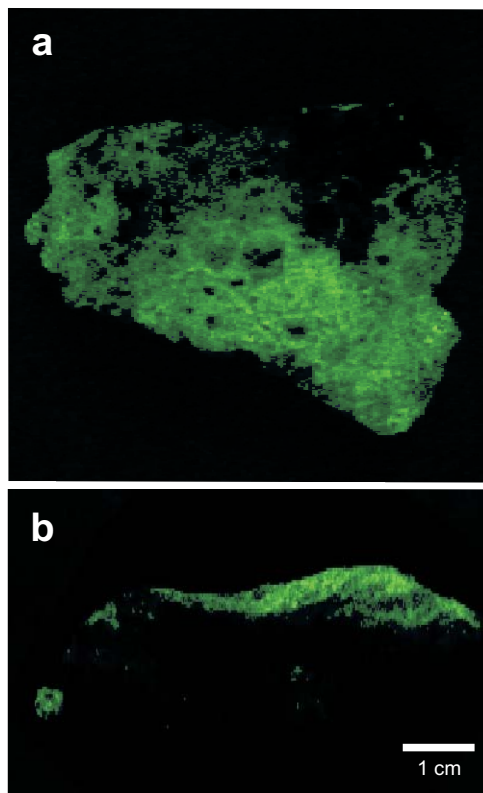


Fig. 6

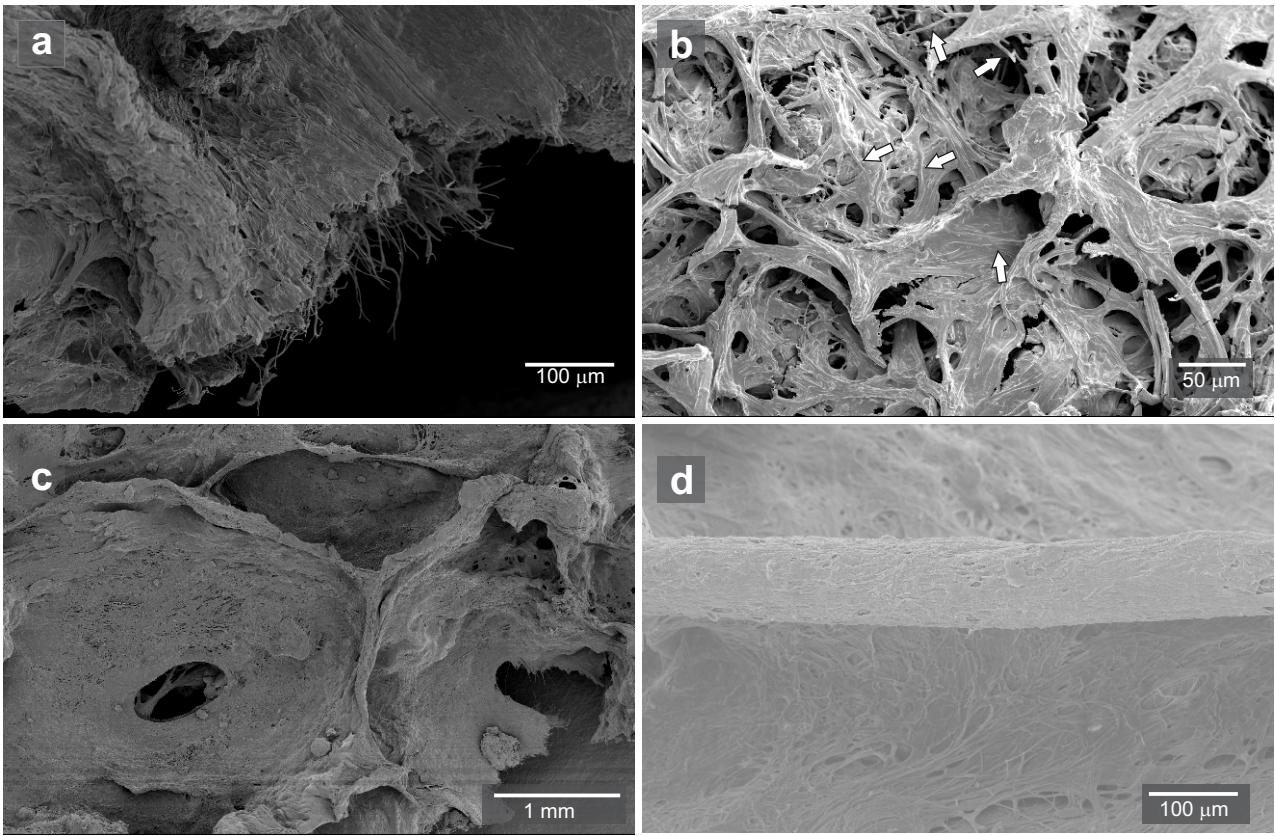


Fig. 7

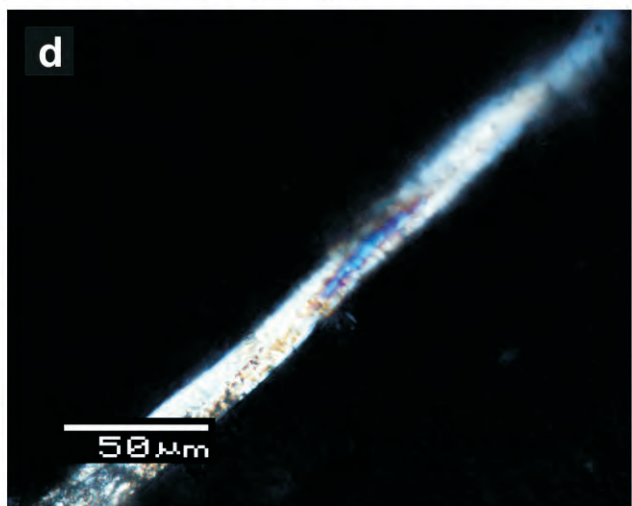
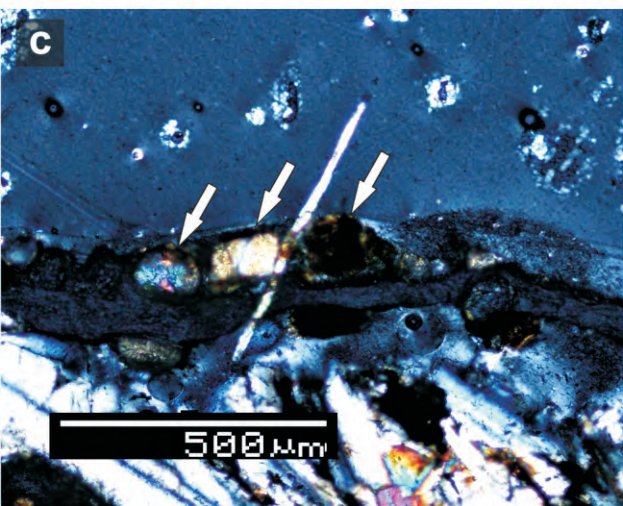
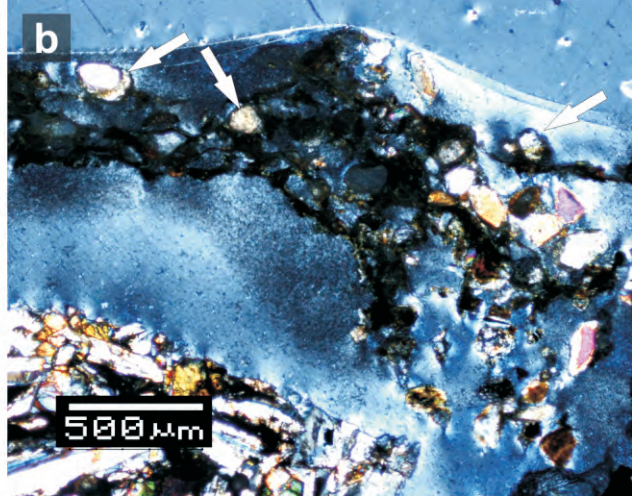
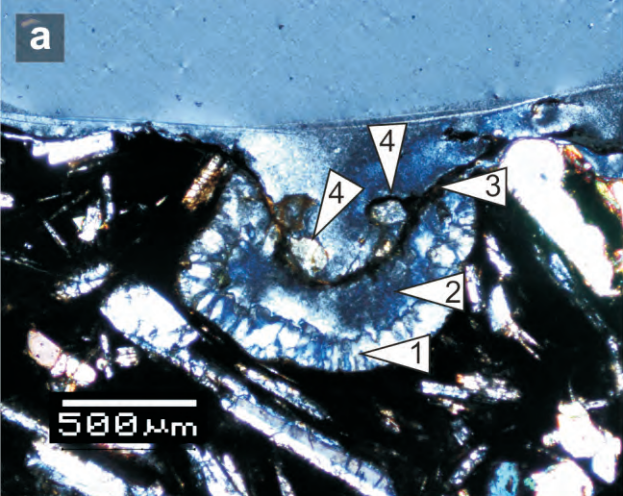


Fig. 8

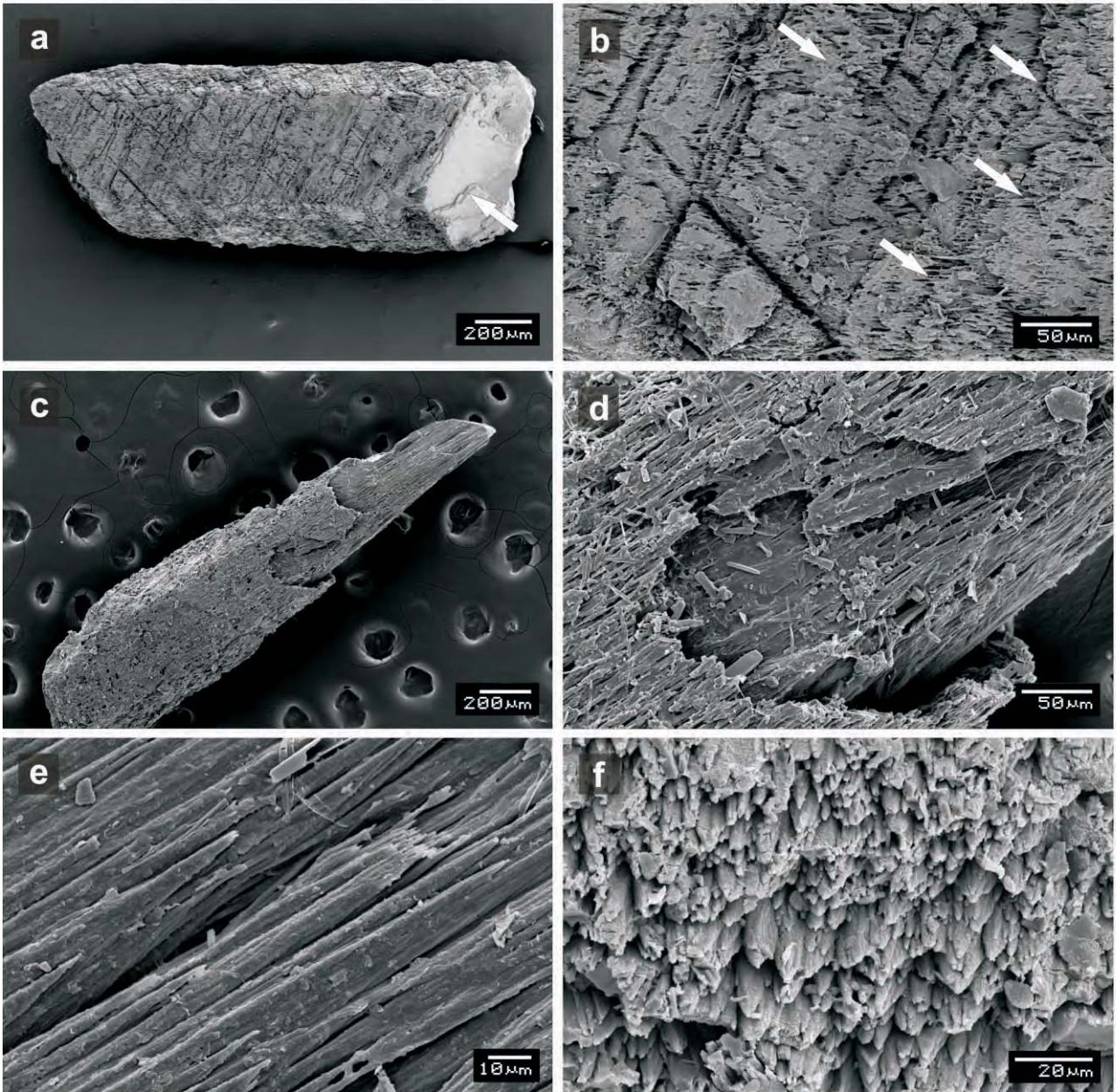


Fig. 9

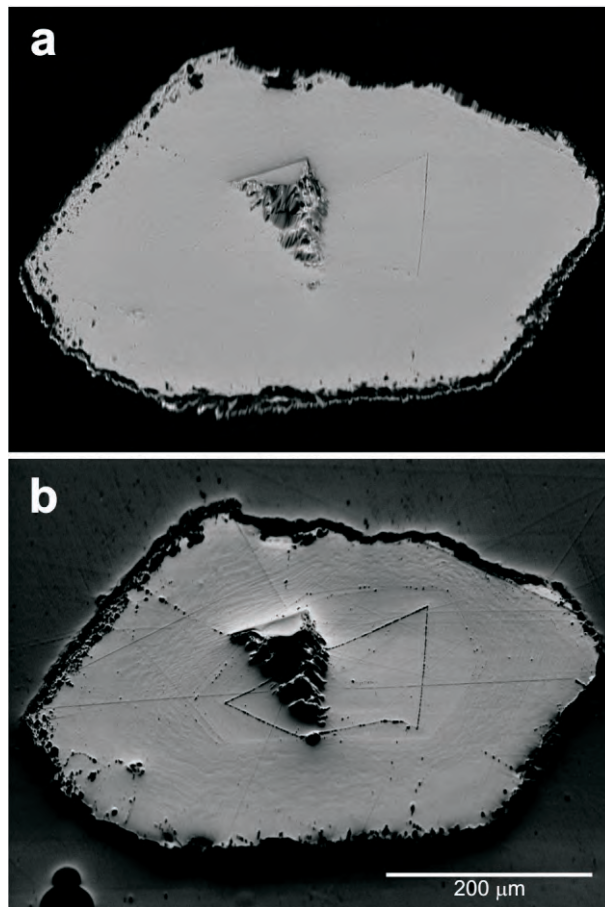


Fig. 10